

AD-A040 835    NAVAL SURFACE WEAPONS CENTER WHITE OAK LAB SILVER SP--ETC F/G 9/5  
HUGGIN'S SCANNED RADIOMETER.(U)  
FEB 77 A D KRALL, J G SCHOFIELD

UNCLASSIFIED

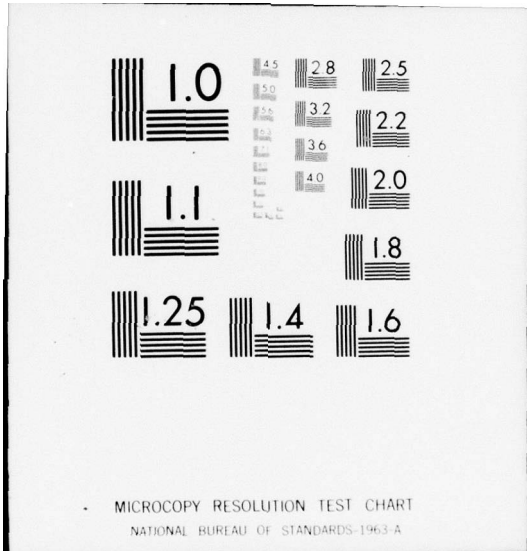
NL

1 of 1  
ADA 040835



END

DATE  
FILMED  
7 - 77



ADA 040835

NSWC/WOL/TR 77-33

NSWC/WOL/TR 77-33

# NSWC

**TECHNICAL  
REPORT**

WHITE OAK LABORATORY

HUGGIN'S SCANNED RADIOMETER

BY  
A.D. Krall  
J.G. Schofield

FEBRUARY 1977

NAVAL SURFACE WEAPONS CENTER  
WHITE OAK LABORATORY  
SILVER SPRING, MARYLAND 20910

- Approved for public release; distribution unlimited.



AD Nu.  
\_\_\_\_\_  
DDC FILE COPY

NAVAL SURFACE WEAPONS CENTER  
WHITE OAK, SILVER SPRING, MARYLAND 20910

## UNCLASSIFIED

SECURITY CLASSIFICATION OF THIS PAGE (When Data Entered)

REPORT DOCUMENTATION PAGE		READ INSTRUCTIONS BEFORE COMPLETING FORM	
1. REPORT NUMBER NSWC/WOL/TR 77-33		2. GOVT ACCESSION NO. <i>90 Technical rept.</i>	
4. TITLE (and Subtitle) Huggin's Scanned Radiometer.		5. TYPE OF REPORT & PERIOD COVERED R&D TQ76 FY77	
6. AUTHOR(s) A. D. Krall, J. G. Schofield		7. PERFORMING ORG. REPORT NUMBER F34-343 IED WA02AE	
9. PERFORMING ORGANIZATION NAME AND ADDRESS Naval Surface Weapons Center White Oak Laboratory White Oak, Silver Spring, Maryland 20910		10. PROGRAM ELEMENT, PROJECT, TASK AREA & WORK UNIT NUMBERS 62332N; F34-343; WF32-343-XXX, WA97XX-30;	
11. CONTROLLING OFFICE NAME AND ADDRESS		12. REPORT DATE February 1977	
14. MONITORING AGENCY NAME & ADDRESS (if different from Controlling Office)		15. SECURITY CLASS. (of this report) UNCLASSIFIED	
16. DISTRIBUTION STATEMENT (of this Report) Approved for public release; distribution unlimited		17. DISTRIBUTION STATEMENT (of the abstract entered in Block 20, if different from Report)	
18. SUPPLEMENTARY NOTES This research was sponsored by NAVAIRSYSCOM and Independent Exploratory Development NSWC/WOL.			
19. KEY WORDS (Continue on reverse side if necessary and identify by block number) Radiometer Electronic Scanned Antenna Millimeter Waves Upconverter Huggins Scanner			
20. ABSTRACT (Continue on reverse side if necessary and identify by block number) Application of Huggins Scanning Technique to a Millimeter Radiometer. Noise calculations are made from the antenna terminals to the IF. A method of providing wide instantaneous bandwidth is discussed, along with a method of beam control.			

391596

Dated

NSWC/WOL/TR 77-33

February 1977

NSWC/WOL/TR 77-33

HUGGIN'S SCANNED RADIOMETER

This report documents the investigation by the NSWC on the application of a Huggin's scanning array to a 35GHz radiometer receiver. The desired performance specifications and directions were provided by NWC, China Lake. The work covers a theoretical study of the feasibility of this scanning technique. Initial funding was supplied by NAVAIRSYSCOM AIR 370D and final funding by Independent Exploratory Development Project WA02AE NSWC/WO. The authors greatly acknowledge the support and assistance received from Mr. J. Vranish, WA-32.

*Paul R. Wessel*

PAUL R. WESSEL  
By direction

1453 for	
IS	White Section <input checked="" type="checkbox"/>
S	Buff Section <input type="checkbox"/>
ANNOUNCED	
STIFICATION.....	
BY	
DISTRIBUTION/AVAILABILITY CODES	
DISC	AVAIL. AND OR SPECIAL
A	

## TABLE OF CONTENTS

	Page
LIST OF TABLES . . . . .	3
LIST OF FIGURES . . . . .	3
I. INTRODUCTION . . . . .	4
II. UPPER SIDEBAND UPCONVERTER . . . . .	8
III. RECEIVER NOISE TEMPERATURE . . . . .	14
IV. A SIMPLE SCANNING ARRAY . . . . .	17
V. THE HUGGIN'S SCANNING ARRAY . . . . .	20
VI. DISCUSSION . . . . .	24
VII. APPENDIX A . . . . .	25

NSWC/WOL/TR 77-33

LIST OF TABLES

Table	Title	Page
1	Radiometer Desired Performance	7
2	Uppersideband Upconverter Performance	13

LIST OF FIGURES

Figure	Title	Page
1	Passive Scanning Antenna	5
2	Frequency Channels of the USUC	12
3	Simplified Radiometer Block Diagram	15
4	Tapped Delay Line	18
5	Series Frequency Scanner Producing Constant I.F. Channel	19
6	Huggin's Scanner	21

## I. INTRODUCTION

This report discusses the application of the Huggin's Scanning system to an electronically scanned antenna receiving array which will then be considered as a radiometer. The desired performance specifications for the system were furnished by R. P. Moore, NWC, China Lake and are listed in Table 1.

The Huggin's Scanning system produces an array of outputs corresponding to the outputs from an antenna array. The outputs of the Huggin's system have a simple controllable progressive phase shift associated with them that is the negative of the progressive phase shift produced by some incoming signal at the antenna terminals. Combining these two signals in an array of non-linear elements can yield an array of outputs proportional to the antenna signals but whose phases are all the same. This array of signals can then be summed into one signal in a corporate combiner and operated on by normal receiving techniques. Incoming signals to a radiometer antenna arrive from all angles but each direction has a uniquely defined progressive phase across the aperture. It is thus the function of Huggin's array control to determine which incoming angle is coherently combined at the output. The control is a variable frequency that can be made as accurate as the application requires. Variation of the control frequency produces the electric scanning of space required by the radiometer.

The array of non-linear elements replace the diode or ferrite phase shifters commonly used in electronically steered antennas and perform much the same function. Figure 1 is an artist's conception of the antenna. The possible advantage to the radiometer is one of system noise. The non-linear elements are capable of performing their function with the addition of a minimum of excess noise. In certain modes they can add gain to the signals and thereby decrease

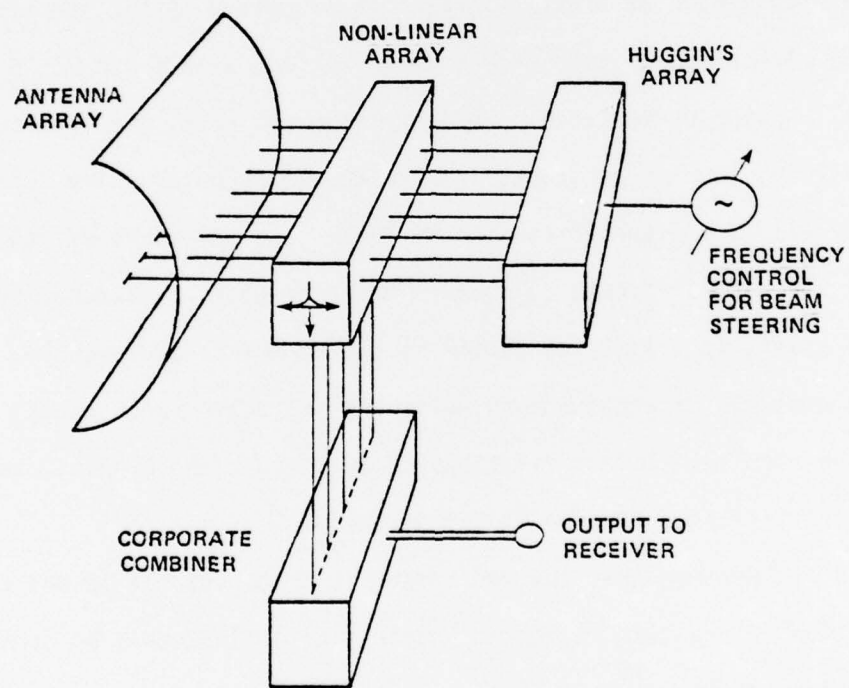


FIG. 1 PASSIVE SCANNING ANTENNA

the effect of noise added by succeeding stages. Gain comes with the price of instability. Because the beam width of Table 1 ( $<0.8^\circ$ ) will require in excess of one hundred elements, stability and low noise were emphasized over gain. The upper-sideband up-converter (USUC), a stable positive resistance mode of a varactor diode was chosen for the application. The analysis, compromises, and constraints result in a circuit that has an effective input noise temperature of  $106^\circ\text{K}$  with a gain of 0.97. It has been suggested that a negative resistance device with a modest gain of 6dB could be made stable and would improve the overall system performance. While this may be true, the absence of experience in building such an array has lead to the more conservative approach.

Of all of the specifications in Table 1, a bandwidth of  $>600\text{MHz}$  appeared to be the most difficult to meet. The array antenna, steered by  $2\pi$  modular phase shift, is a limiting factor to the bandwidth achievable. Much of our early work was directed toward solving this problem and several schemes appeared to show promise. Time limitations dictated that the emphasis be placed on the characteristics of the non-linear varactors.

It was assumed that the radiometer is to be scanned in one direction and that formation of the beam in the non-scanned direction would be done with a parabola. Regardless of how this is to be accomplished, this report considers that there will be some  $n$  output ports available from a linear array that are to be electronically scanned.

Table 1  
RADIOMETER DESIRED PERFORMANCE

## ARRAY

Size	36" x 36"
Beam Angle from Broadside	0
Type	NP
Builder	NP
MAXIMUM SCAN SPEED	60/Sec
SCAN ANGLE	> 100°
SYSTEM BANDWIDTH (3 dB)	> 600 MHz
GAIN	> 70dB
BEAM SPREAD TO EDGE OF SCAN	< 2:1
SYSTEM NOISE FIGURE	
With Radiometric Amplifier (2.5 dB)	< 6 dB
For Scan System Only	< 1 dB
SYSTEM LOSS (Include dissipation and VSWR's)	< 2 dB
EFFICIENCY (Amount of energy reaching detector compared to standard antenna)	> 70%
SIDELOBE LEVELS	
First Sidelobe	< -22 dB
Average Sidelobe	< -30 dB
BEAMWIDTH	< 0.8°
Dimensions	36" x 36" x 4"
Weight	< 75 lbs.
POWER	< 200 W
NP - No Preference	

## II. UPPER SIDEBAND UP-CONVERTER

The building block of the array scanner is a varactor diode operating as a nonlinear capacitor in the upper sideband up-converter mode. It has as its inputs, the signal from the antenna port ( $f_1$ ) and a pump signal ( $f_2$ ) purposefully inserted to vary or pump the nonlinear capacitance. Because of the nonlinearity these signals will, in general, generate a set of frequencies equal to  $mf_1 + nf_2$ , where  $m$  and  $n$  are integers. In an ideal case the power flow at the various frequencies is governed by the Manley-Rowe equations written as

$$\sum_{m=0}^{\infty} \sum_{n=0}^{\infty} \frac{mP_{mn}}{mf_1 + nf_2} = 0 \quad (1)$$

$$\sum_{n=0}^{\infty} \sum_{m=0}^{\infty} \frac{nP_{mn}}{mf_1 + nf_2} = 0 \quad (2)$$

By assuming circuit conditions such that power can flow only at frequencies  $f_1$ ,  $f_2$ , and  $f_3$  where  $f_1 + f_2 = f_3$  (the upper sideband up-converter mode) the above equations reduce to

$$\frac{1 P_{1,0}}{1 f_1} + \frac{1 P_{1,1}}{1f_1 + 1f_2} = \frac{P_1}{f_1} + \frac{P_3}{f_3} = 0 \quad (1a)$$

$$\frac{1 P_{0,1}}{1 f_2} + \frac{1 P_{1,1}}{1 f_1 + 1 f_2} = \frac{P_2}{f_2} + \frac{P_3}{f_3} = 0 \quad (2a)$$

From equation 2a it can be seen that when the pump power  $P_2$  is applied to the diode ( i.e.  $P_2$  is positive), then  $P_3$  is negative.  $P_3$  is supplied by the diode at frequency  $f_3$ . A negative  $P_3$  in equation 1a is also consistent with a positive  $P_1$  (the antenna signal) and therefore both inputs have positive resistance. The device is stable, the main reason for choosing this mode.

The maximum available power gain  $\frac{P_3}{P_1}$  is given by equation 1a as  $f_3/f_1$  where  $f_3 > f_1$ . Because the signal frequency  $f_1$  is 35GHz, the gain will be limited by not allowing  $f_3$  to exceed practical circuit capabilities.

Thermal noise is introduced via the series resistance of the varactor diode. Following the analysis of Penfield & Rafuse, the expression for the optimized noise temperature is given by.

$$T_a = T_d \left\{ \frac{2f_1}{m_1 f_c} \left[ \frac{f_1}{m_1 f_c} + \sqrt{1 + \left( \frac{f_1}{m_1 f_c} \right)^2} \right] \right\} \quad (3)$$

where

$T_a$  = effective diode noise temperature

$T_d$  = diode junction temperature

$f_1$  = 35GHz

$f_c$  = diode cutoff frequency

$m_1$  = pumping parameter

This equation is independent of the pump frequency  $f_2$  and the output frequency  $f_3$ . It can therefore be used to determine the proper varactor diode and the method of pumping which are incorporated in the term  $m_1 f_c$ . Since  $m_1 f_c$  is in the denominator it should be maximized to reduce the apparent noise temperature. It also turns out that a maximum  $m_1 f_c$  will reduce the diode junction temperature. The parameter  $m_1$  can have a value of 0.25 if we choose an abrupt junction varactor and pump it with a sinusoidal current. The cutoff frequency  $f_c$  of the diode is a function of the junction capacitance and the series resistance. Picking an epitaxial GaAs varactor, a value of  $f_c = 900\text{GHz}$  is possible.

The gain of the up-converter is given as

$$G = \frac{\left[ 1 + \left( \frac{m_1 f_c}{f_1} \right)^2 \right]^{1/2}}{\left[ \frac{f_1}{m_1 f_c} + \sqrt{1 + \left( \frac{f_1}{m_1 f_c} \right)^2} \right] \left[ \frac{f_1}{m_1 f_c} + \sqrt{1 + \left( \frac{f_1}{m_1 f_c} \right)^2} + \frac{m_1 f_c}{f_3} \right]} \quad (4)$$

which from previous constraints reduces to

$$G = \frac{6.51}{1.17 \left( 1.17 + \frac{225}{f_3} \right)} \quad (4a)$$

Choosing  $f_3 \rightarrow \infty$  results in a maximum gain of 6.8dB for this case. However, choosing the output frequency  $f_3$  also specifies the pump frequency  $f_2$  since  $f_1 + f_2 = f_3$ .

The choice of values for  $f_2$  or  $f_3$  must be based on other considerations than gain. The pump frequency  $f_2$  is related to the power required to pump the varactor diode. For a fully pumped (sinusoidal current) abrupt junction varactor the power required is

$$P \text{ (watts)} \approx 12.5 \left( \frac{f_2}{f_c} \right)^2 \quad (5)$$

Equation 5 indicates that as  $f_2$  increases the required pump power will increase. An increase in pump power will produce an increase in the junction temperature which from Equation 3 will increase the noise temperature. It will also decrease the diode life (MTBF). In general the low pump frequencies are advantageous except for gain. One more constraint on the choice of pump frequency is the circuit. Earlier it was assumed that power flows through the varactor at  $f_1$ ,  $f_2$  &  $f_3$ . No harmonics or subharmonics are allowed. For the required bandwidth, the separation of allowable frequency bands by simple low loss filter circuits must be physically wide or some overlap is bound to occur. Figure 2 depicts some of the possible channels in which currents might flow. Although there are other possibilities, the pump frequency was chosen as  $f_2 = 14\text{GHz}$ . From Figure 2 it can be seen that this choice will facilitate circuit construction by allowing reasonable band separations. Choosing  $f_2$  automatically fixes the output frequency  $f_3 = 49\text{GHz}$ . The effective noise temperature  $T_a$  (Equation 3), the gain  $G$  (Equation 4a) and the pump power (Equation 5) can now be calculated and for this case are tabulated in Table 2.

NSWC/WOL/TR 77-33

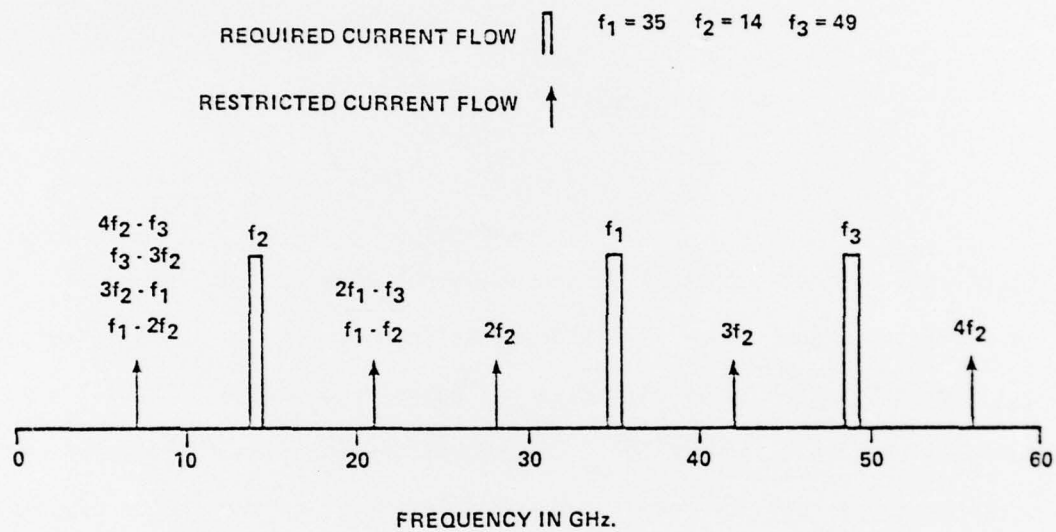


FIG. 2 FREQUENCY CHANNELS OF THE USUC

TABLE 2  
UPPERSIDEBAND UPCONVERTER PERFORMANCE

$$T_a - T_d \times 0.36 = 106^\circ K \quad \text{where } T_d = 292^\circ K$$

$$G = 0.97 = 0.13 \text{dB loss}$$

$$P_{f_2} = 3 \text{mW}$$

To justify taking the diode junction temperature as  $292^\circ K$ , the assumption is that this diode operates similarly to others. It has been shown that a  $7\mu m$  GaAs Schottky Barrier diode will have a temperature rise given by

$$\Delta T_j \sim 540 P_{f_2} = 2^\circ K \quad (6)$$

The corresponding MTBF for a  $p^+ n$ -GaAs varactor is given by

$$MTBF \sim 7.7 \times 10^{-7} \exp \frac{1.18 \times 10^5}{T_j} \sim 10^7 \text{ years} \quad (7)$$

Pump power required for the total array at 3mW/stage is less than 1 watt for an array of approximately 128 stages. An additional bias of 2 volts D.C. will be required on the varactors. This then is the basic building block of the array.

## III. THE RECEIVER NOISE TEMPERATURE

With the USUC specified, the effective noise temperature from the antenna terminals to the IF will be estimated. Figure 3 is the block diagram of this portion of the radiometer. The low noise amplifier is inserted after the power combiner to mask the noise of the down converter and the IF. Here only one amplifier is needed and the luxury of a somewhat unstable negative resistance high gain amplifier can be utilized. The numbers assigned are somewhat arbitrary but hopefully reasonable.

The corporate combiner is considered to have 1.5dB loss ( $G_{cc} = 0.71$ ) and by assuming an ambient temperature of  $290^{\circ}\text{K}$  will have an effective temperature of

$$T_{ecc} = \frac{T_{amb} (1-G_{cc})}{G_{cc}} = \frac{290 (1-.71)}{.71} = 118^{\circ}\text{K} \quad (8)$$

An uncooled paramp with a down converter is assumed to have a noise figure of 3dB(2) and a gain of 10dB ( $G_{PADC} = 10$ ).

$$\therefore T_{e_{PADC}} = T_0 (F-1) = 290 (2-1) = 290^{\circ}\text{K} \quad (9)$$

The IF amplifier has a noise figure of 2.5dB (1.78)

$$\therefore T_{e_{IF}} = T_0 (F-1) = 290 (1.78-1) = 226^{\circ}\text{K} \quad (10)$$

The cascade noise temperature of Figure 3 can now be calculated as

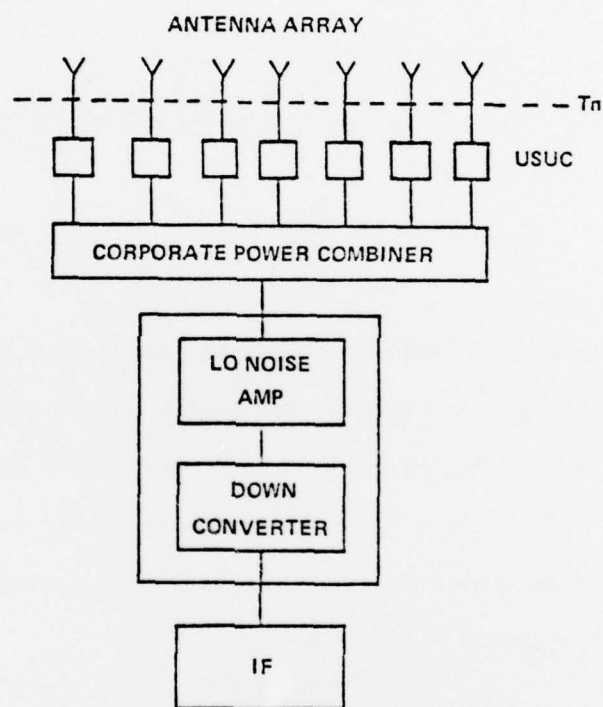


FIG. 3 SIMPLIFIED RADIOMETER BLOCK DIAGRAM

$$\begin{aligned}
 T_n &= T_{auc} + \frac{T_{ecc}}{G_{uc}} + \frac{T_{epadc}}{G_{uc} G_{cc}} + \frac{T_{eif}}{G_{uc} G_{cc} G_{padc}} \\
 &= 106 + \frac{118}{0.97} + \frac{290}{.97 \times .71} + \frac{226}{.97 \times .71 \times 10} \\
 &= 106 + 122 + 421 + 33 = \\
 &= 682^{\circ}\text{K}
 \end{aligned} \tag{11}$$

The noise figure referred to the input terminals of the up-converter is

$$F = \frac{T_n}{T_0} + 1 = \frac{682}{290} + 1 = 3.35 \text{ or } 5.25\text{dB.} \tag{12}$$

From the above equations it can be seen that a simple gain of 2 in the upper sideband up-converter instead of  $G_{uc} = 0.97$  would have reduced the noise figure to 4.2dB. A further reduction of the paramp down converter noise figure to 2dB would then yield a 3.1dB noise figure at the input terminals. Many such speculations have been considered and discarded because they were considered not feasible at the present time.

## IV. A SIMPLE SCANNING ARRAY

In Figure 1 the purpose of the Huggin's array is to provide pump power to the up-converters with a controllable phase difference between adjacent terminals. The easiest way to accomplish this function is with the use of a tapped delay line shown in Figure 4. The delayline is arranged so that at some frequency  $f_2$  each output port is exactly  $2n\pi$  delayed in phase from the preceding port. At  $f_2$  the ports are then effectively at the same phase. As the frequency  $f_2$  is increased or decreased the wavelength on the line will decrease or increase and a progressive phase shift will occur between the ports at this new frequency. The major drawback to this approach is that the instantaneous bandwidth is limited if a narrow beamwidth is required. There is also an aperture effect that puts a restriction on the bandwidth which for scanning from broadside in one direction tends to cancel the limitation of bandwidth caused by frequency scanning. This apparent cancellation was investigated in an effort to obtain the required >600MHz instantaneous bandwidth but no definite conclusions were made.

Figure 5 shows how a series delay line frequency scanner could be implemented to produce a constant IF channel frequency.

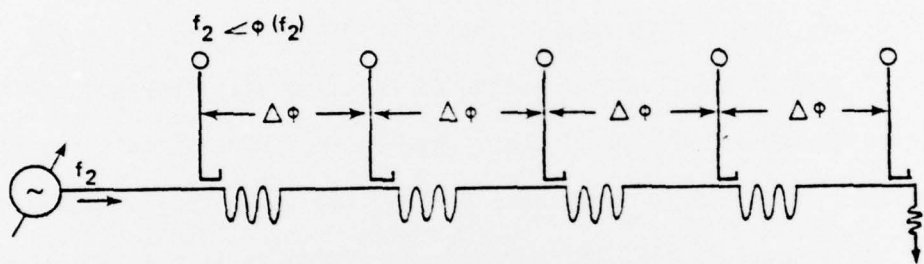


FIG. 4 TAPPED DELAY LINE

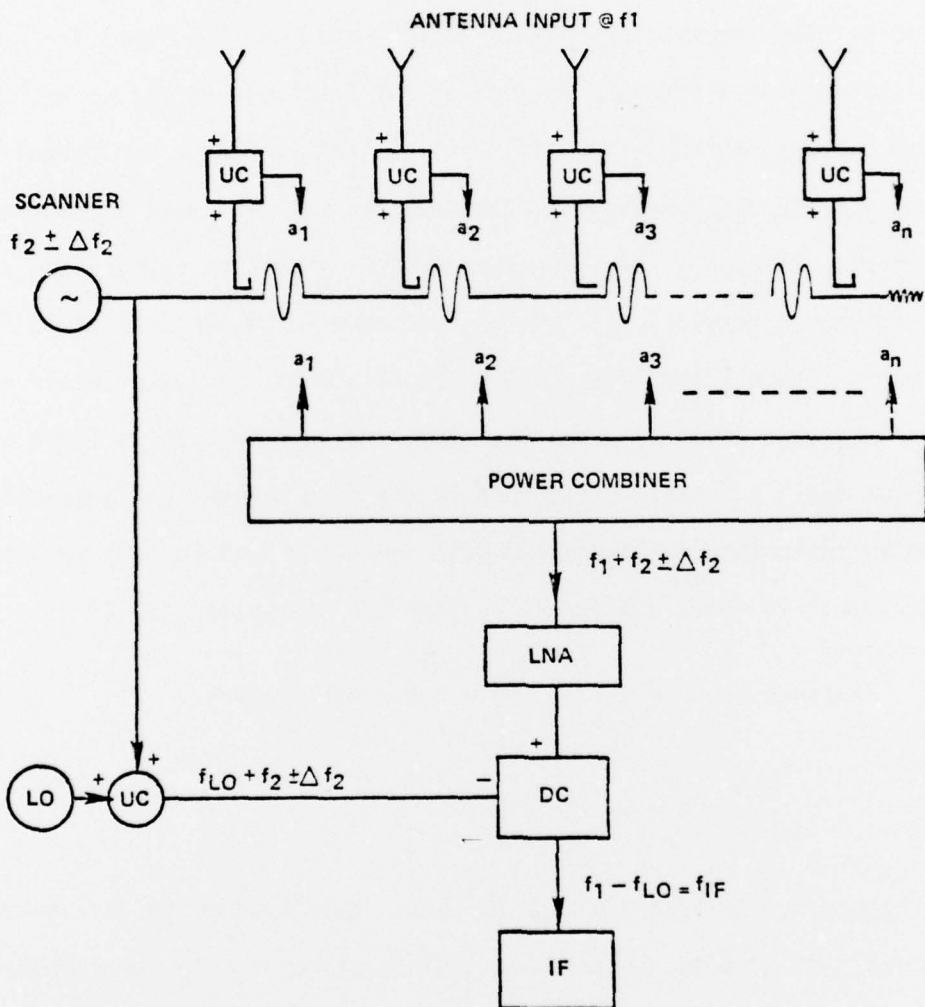


FIG. 5 SERIES FREQUENCY SCANNER PRODUCING CONSTANT I.F. CHANNEL

## V. THE HUGGIN'S SCANNING ARRAY

The Huggin's scanning system is based on the series delay line scanner but has the advantage having a constant output frequency  $f_2$  through all scan angles. Figure 6 is a schematic of the Huggin's scanner. Details of the math are in Appendix A. The important result is that by changing the input frequency  $f_y$  the relative phase difference between output ports can be varied without changing the output frequency. If it is desired to change the output frequency, this can be done by changing  $f_x$  independent of  $f_y$ . The output frequency  $f_2$ , at all ports, is always  $2f_x$ . Two such systems have been constructed at NSWC/WOL with predictable results. If this scanner were to be implemented in the array as shown in Figure 1 the instantaneous bandwidth of the system would be limited by the "aperture effect." That is, since the antenna size is fixed and for a given beam angle the phase difference is fixed, a change in frequency off center frequency (instantaneous bandwidth) will cause the beam to move in space.

The result in numerical terms is, when the beam scans to  $60^\circ$

$$\text{Instantaneous Bandwidth (\%)} = \text{Beamwidth (degrees)} \quad (13)$$

$$\frac{\Delta f}{f_0} \cdot 100 = \theta_0 \text{ (3dB)} \quad (13a)$$

As a radiometer, the instantaneous bandwidth must be limited to keep the beamwidth within its desired size. From Table 1  $\Delta f$  is calculated to be <280MHz which is insufficient.

Suppose now that one sweep of a given terrain is made with the Huggin's array and this information is stored. Then a second sweep is made with the array of the exact same terrain but this time the freq  $f_2$  is shifted by 280MHz.

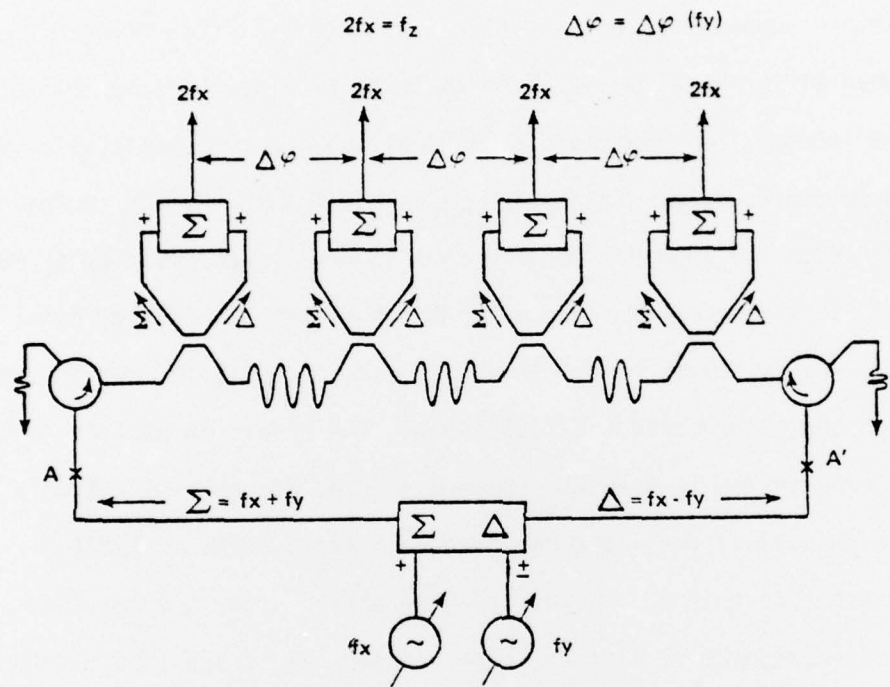


FIG. 6 HUGGINS' SCANNER

If this information is then added to the stored information the effective bandwidth will now be  $2 \times 280 = 560$  MHz. Here bandwidth is traded for time which will not improve the sensitivity of a radiometer since (r.f. bandwidth  $\times$  integration time) is a factor in the sensitivity.

However, suppose  $f_2$  could be simultaneously two frequencies each with their own proper differential phase shift to be looking at the same cell on the ground. Then the integration time could be left at its maximum permissible value and the r.f. bandwidth could be increased. It is similar to stagger tuning an interstage coupler. With the Huggin's scanner this is easily accomplished by duplicating in parallel everything below the points AA' in Figure 6. The low noise amplifier, where the instantaneous bandwidth is limited, must also be duplicated in parallel to accept the second band of frequencies. The extension of this concept to three or more frequencies is straight forward. Three frequencies are more than adequate to satisfy the  $> 600$  MHz bandwidth requirement of Table 1.

One other feature of a planar scanned phased array antenna that is bothersome to systems designers is that the beam broadens as it scans away from broadside. For an aperture large compared to wavelength and a scan angle from broadside  $\theta_0 < 60^\circ$  an approximate expression for beamwidth is

$$\theta_{3dB} \text{ (Scanned to } \theta_0) = \frac{\theta_{3dB} \text{ (measured at broadside)}}{\cos \theta_0} \quad (14)$$

The Huggin's array can be arranged so that the beamwidth will remain constant through all angles. Viewing the problem backwards, it could be said that the beam tends to narrow as it approaches broadside. That being the case, the problem then is to broaden the beam electronically. The control frequency  $f_y$

of the Huggin's scanner determines the position of the beam in space. If  $f_y$  is composed of two frequencies,  $f_{y_1}$  and  $f_{y_2}$ , there will then be two simultaneous beams defined in space. When  $f_{y_1}$  and  $f_{y_2}$  are closely spaced in frequency, the beams will overlap and appear to be one broadened beam in space. As the frequencies are made to converge to  $f_y$ , the beam will narrow to the width defined by the aperture. By controlling the convergence of  $f_{y_1}$  and  $f_{y_2}$  to be a function of  $\cos\theta_0$ , the array effect of Equation 14 can be cancelled and the beam size remains constant over all scan angles. Again the extension to more than two frequencies ( $f_{y_1}$ ,  $f_{y_2}$ ,  $f_{y_3}$  ...) is straight forward. The control of the beamwidth by  $f_2$  has the same action as a zoom lens camera. Utilizing this procedure requires an increase in array size to produce a given beamwidth at broadside.

## VI. DISCUSSION

In a radiometer application the Huggin's array utilized as the pump for an array of unconverters has some definite advantages. The low noise capability of the upconverters in a system has been calculated and the flexible control of the Huggin's array as the pump has been demonstrated. Modifications of the two simple frequency controls lead to an increase in signal bandwidth and beam shape control.

The outstanding question is, can these numbers be reproduced in hardware performance at 35 GHz and at an affordable price. The Huggin's array has a maximum frequency of 14GHz at its output but most of its signals are below half this value. Since transmission losses in this region are reasonably low no special difficulties are apparent. The upconverters operate at a maximum freq of 49GHz where line losses are very serious, especially for low noise circuits. It is therefore suggested that the upconverters performance in practice be demonstrated as a next step. From there a more realistic performance and price could be determined.

## VII. APPENDIX A

Referring to Figure 6 the input frequency  $f_x$  and  $f_y$  can be written as

$$f_x = X \sin (\omega_{xt} + \phi_x) \quad (15)$$

$$f_y = Y \sin (\omega_{yt} + \phi_y) \quad (16)$$

These frequencies are mixed to form the sum ( $\Sigma$ ) and ( $\Delta$ ) which are separated and directed to travel opposite directions on the delay line. The sum and difference signals can be written as

$$\Sigma = A \sin (\omega_x + \omega_y)t + \phi_x + \phi_y \quad (17)$$

$$\Delta = B \sin (\omega_x - \omega_y)t + \phi_x - \phi_y \quad (18)$$

The power couplers for the sum channel are assumed to couple only signals traveling in the sum direction and are placed symmetrically along the delay line. The same is true of the difference couplers. At any two arbitrary and neighboring sets of couplers labeled  $n$  and  $n+1$  the sum channel can be written as

$$\text{Coupler } n \quad \Sigma_n = A' \sin (\omega_x + \omega_y)t + \phi_n \quad (19)$$

$$\text{Coupler } n+1 \quad \Sigma_{n+1} = A'' \sin (\omega_x + \omega_y)t + \phi_n + \phi_\Sigma \quad (20)$$

where  $\phi_\Sigma$  is the phase change resulting from the delay path ( $d$ ) between the couplers and is given by

$$\phi_\Sigma = \frac{d}{v} (\omega_x + \omega_y) \quad (21)$$

Assuming that the difference channel  $\Delta$  travels the delay line with the same velocity as the sum channel but in the opposite direction then at the couplers it can be written as

$$\Delta_{n+1} = B' \sin (\omega_x - \omega_y)t + \phi'_n \quad (22)$$

$$\Delta_n = B'' \sin (\omega_x - \omega_y)t + \phi'_n + \phi_\Delta \quad (23)$$

$$\text{where } \phi_\Delta = \frac{d}{v} (\omega_x - \omega_y) \quad (24)$$

{}

Since the paths that each signal follows from the couplers to the upconverters is symmetrical the foregoing expressions can be utilized as the inputs to the up-converters. The up-converters act as a non-linear mixers where the sum frequencies of their respective inputs are separated as outputs. The outputs  $n$  and  $n+1$  can be written as.

$$\text{Output } n = C \sin [(\omega_x + \omega_y)t + \phi_n + (\omega_x - \omega_y)t + \phi'_n + \phi_\Delta]$$

$$= C \sin [2\omega_x t + \phi_n + \phi'_n + \phi_\Delta] \quad (25)$$

$$\text{Output } n+1 = C' \sin [(\omega_x + \omega_y)t + \phi_n + \phi_\Sigma + (\omega_x - \omega_y)t + \phi'_n]$$

$$= C' \sin [2\omega_x t + \phi_n + \phi'_n + \phi_\Sigma] \quad (26)$$

The amplitudes C & C' can be adjusted to be equal, independently of frequency and phase. Both outputs n and n+1 have the frequency  $f_2 = 2fx$  and thus fx is the frequency control. The difference in phase between the two adjacent ports can be seen to be

$$\Delta_\phi = \phi_\Sigma - \phi_\Delta = \frac{d}{v} 2\omega_y = \frac{4\pi d}{v} fy \quad (27)$$

The frequency control of fy is therefore the beam steering control of the array.

NSWC/WOL/TR 77-33

DISTRIBUTION

	Copies
Commander Naval Weapons Center China Lake, CA 93555 Attn: R. P. Moore (Code 3542) G. Ryno (Code 3313) J. Blair (Code 2608)	5 1 1
Commander Naval Air Systems Command Washington, D.C. 20361 AIR 370D (E. T. Hooper, Jr.) AIR 03P2 (J. W. Malloy)	3 1
Commander Naval Sea Systems Command Washington, D.C. 20362 SEA 03B SEA 03411 (T. Tasaka) SEA 03412 (J. H. DeMattia)	1 1 1
SAMSO/RSMG Air Force Systems Command Los Angeles, CA 90009 Attn: Lt. J. P. Rouge	1
Defense Documentation Center Cameron Station Alexandria, Virginia 22314	12